



## Get Clarity On Generics

Cost-Effective CT & MRI Contrast Agents

**FRESENIUS  
KABI**

[WATCH VIDEO](#)

# AJNR

## **Assessment of the Membranous Labyrinth in Infants Using a Heavily T2-weighted 3D FLAIR Sequence without Contrast Agent Administration**

G. Conte, S. Casale, L. Caschera, F.M. Lo Russo, C. Paolella, C. Cinnante, F. Di Berardino, D. Zanetti, D. Stocchetti, E. Scola, L. Bassi and F. Triulzi

This information is current as of August 11, 2025.

*AJNR Am J Neuroradiol* 2021, 42 (2) 377-381

doi: <https://doi.org/10.3174/ajnr.A6876>

<http://www.ajnr.org/content/42/2/377>

# Assessment of the Membranous Labyrinth in Infants Using a Heavily T2-weighted 3D FLAIR Sequence without Contrast Agent Administration

 G. Conte,  S. Casale,  L. Caschera,  F.M. Lo Russo,  C. Paoletta,  C. Cinnante,  F. Di Bernardino,  D. Zanetti,  D. Stocchetti,  E. Scola,  L. Bassi, and  F. Triulzi



## ABSTRACT

**BACKGROUND AND PURPOSE:** Imaging is fundamental to assessing the acoustic pathway in infants with congenital deafness. We describe our depiction of the membranous labyrinth in infants using the heavily T2-weighted 3D FLAIR sequence without a contrast agent.

**MATERIALS AND METHODS:** We retrospectively reviewed 10 infants (20 ears) (median term equivalent age: 2 weeks; IQR: 1–5 weeks) who had undergone brain MR imaging including a noncontrast heavily T2-weighted 3D FLAIR scan of the temporal bone. For each ear, 3 observers analyzed, in consensus, the saccule, the utricle, and the 3 ampullae, assessing the visibility (score 0, not appreciable; score 1, visible without well-defined boundaries; score 2, visible with well-defined boundaries) and morphology (“expected” or “unexpected” compared with adults). The heavily T2-weighted 3D FLAIR sequence was scored for overall quality (score 0, inadequate; score 1, adequate but with the presence of image degradation; score 2, adequate).

**RESULTS:** Six (60%) MR examinations were considered adequate (score 1 or 2). The saccule was visible in 10 ears (83.3%) with an expected morphology in 9 ears (90%). In 1 ear of an infant with congenital deafness, the saccule showed an unexpected morphology. The utricle was visible as expected in 12 ears (100%). The lateral ampulla was visible in 5 ears (41.6%), the superior ampulla was visible in 6 ears (50.0%), and the posterior ampulla was visible in 6 ears (50.0%), always with expected morphology (100%).

**CONCLUSIONS:** MR imaging can depict the membranous labyrinth in infants using heavily T2-weighted 3D FLAIR without an injected contrast agent, but the sequence acquisition time reduces its feasibility in infants undergoing MR studies during natural sleep.

**ABBREVIATION:** HT2W = heavily T2-weighted

Congenital bilateral permanent hearing loss is a chronic condition affecting approximately 1.33 per 1000 live births.<sup>1,2</sup> Environmental and prenatal factors such as congenital infections, particularly cytomegalovirus, are common risk factors, most notably in low-income settings.<sup>3</sup> Genetic causes account for most cases in developed countries and can lead to syndromic and nonsyndromic congenital hearing loss.<sup>4–6</sup> Hearing during the critical periods of infancy and early childhood is necessary to develop spoken

language.<sup>7</sup> Thus, hearing screening tests are performed no later than the first month of age.<sup>8</sup> If congenital hearing loss is detected, understanding the cause is necessary to direct therapeutic decision making and guide prevention and (genetic) counseling.

Imaging plays a fundamental role in the assessment of the congenital hearing loss by detecting malformations, guiding genetic testing, helping to diagnose congenital cytomegalovirus infection, and providing preoperative information, including the feasibility of cochlear implantation and surgical risk factors.<sup>2</sup> Although CT is the imaging technique of choice for assessing the bony labyrinth and MR imaging is fundamental to evaluating the cochlear nerve and CNS in children and adults,<sup>9–11</sup> no imaging study has been used to visualize the membranous labyrinth in infants.

Heavily T2-weighted (HT2W) 3D FLAIR images acquired 4 to 5 hours after IV contrast agent administration can assess the membranous labyrinth in adults.<sup>12,13</sup> However, this imaging protocol may not be suitable for infants because of the need for contrast agent injection and to acquire the images during

Received May 16, 2020; accepted after revision September 1.

From the Neuroradiology Unit (G.C., S.C., L.C., F.M.L.R., C.C., D.S., E.S., F.T.), Audiology Unit (F.D.B., D.Z.), and NICU (L.B.), Fondazione IRCCS Ca' Granda Ospedale Maggiore Policlinico Milano, Università degli Studi di Milano, Milan, Italy; Department of Advanced Biomedical Sciences (C.P.), University of Naples “Federico II,” Naples, Italy; and Department of Pathophysiology and Transplantation (F.T.), University of Milan, Milan, Italy.

Please address correspondence to Luca Caschera, MD, Fondazione IRCCS Ca' Granda Ospedale Maggiore Policlinico, Neuroradiology Unit, Via Francesco Sforza 35, Milan, Italy; e-mail: luca.caschera@policlinico.mi.it; @caschera\_luca; @GiorgioConte86



Indicates article with supplemental online photo.

<http://dx.doi.org/10.3174/ajnr.A6876>

separate sessions. In this study, we describe our experience in depicting the normal anatomy of the membranous labyrinth in a cohort of infants using the HT2W 3D FLAIR sequence with no contrast agent.

## MATERIALS AND METHODS

### Participants

This is a retrospective observational study approved by the institutional review board. Infants were recruited as clinical cases with ethical approval for review of clinical notes and MR images with consent from parents or legal guardians. The cohort consists of infants who underwent brain MR imaging with HT2W 3D FLAIR of the temporal bone at our neuroradiology department from September 2019 to January 2020. All brain MR imaging was performed for clinical purposes, and the HT2W 3D FLAIR sequence was acquired as part of the optimization of MR imaging protocols after the upgrade of the MR imaging scanner. Infants were not consecutively enrolled because the HT2W 3D FLAIR sequence was performed when a neuroradiologist with expertise in head and neck radiology (G.C.) was overseeing the MR imaging session. No exclusion criteria were adopted.

### MR Imaging Acquisition

Each participant was imaged on a 3T Achieva scanner (Philips Healthcare) using a 32-channel phased-array coil. We applied a scan-specific energy dose corresponding to 0.5 kJ/kg that varied according to the baby's weight. Small infants (younger than 3 months of age) were scanned during natural sleep after feeding or under sedation with oral midazolam. One patient (23 months of age) was scanned under sedation with propofol. During the MR examination, infants were monitored by pulse oximetry and electrocardiography (Invivo-Expression Monitor MR200). Small infants (younger than 3 months of age) were also dressed in MR-compatible tracksuits; a warm blanket and a hat were used to prevent heat dispersion.<sup>14</sup> Appropriate noise attenuators (MiniMuffs, Natus Medical) were used.

The imaging protocol consisted of sequences performed for whole-brain evaluation: T1-weighted 3D fast field-echo sequence, axial and coronal T2-weighted turbo spin-echo sequences, axial DWI sequence, and axial SWI sequence. The HT2W 3D FLAIR sequence was used to evaluate the membranous labyrinth with the following parameters: axial plane; TR: 6000 ms; TE: 350 ms; TI: 2350 ms; fat saturation: spectral presaturation with inversion recovery; TSE factor: 182; flip angle: 90 degrees; number of slices: 30; FOV:  $230 \times 190 \text{ mm}^2$ ; matrix:  $232 \times 229$ ; voxel size:  $0.7 \times 0.7 \times 0.7 \text{ mm}^3$ ; averages: 6; and scan time: 10 minutes and 6 seconds. Because MR examination was performed for clinical purposes, the HT2W 3D FLAIR sequence was acquired only at the end of the MR protocol. This guaranteed the best quality of MR images acquired for diagnostic purposes, an acceptable scanning time, and the shortest sedation time when applicable. Of note, sedation was never prolonged to obtain good-quality HT2W 3D FLAIR images. No contrast agent was injected during the examinations.

### Image Analysis

Three observers (1 senior neuroradiologist with 10 years of experience in neuroimaging and 2 young neuroradiologists with 2 years

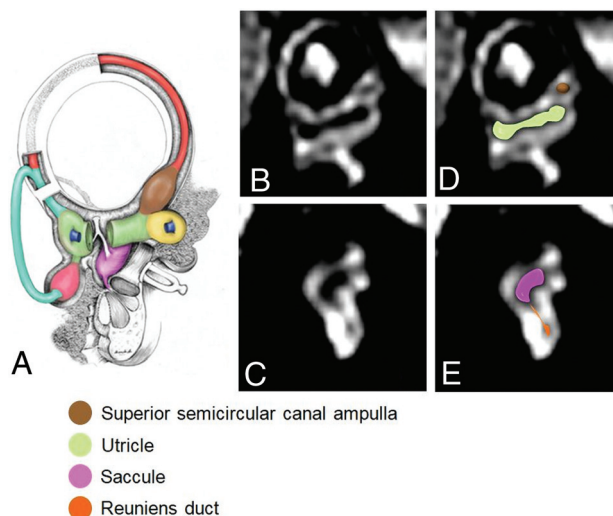


**FIG 1.** Schematic representation of the membranous labyrinth in the sagittal plane parallel to the superior semicircular canal (A, asterisk) and corresponding reformatted oblique sagittal MR images (B, intermediate sagittal plane; C, medial sagittal plane) with the corresponding colored representational structures (D and E). In E, the reuniens duct connecting the inferior portion of the saccule and the cochlear duct is highlighted in orange. The images were obtained from the same participant. (Reprinted from Conte G, Caschera L, Tuscano B, et al. Three-Tesla magnetic resonance imaging of the vestibular endolymphatic space: a systematic qualitative description in healthy ears. *Eur J Radiol* 2018; 109: 79. Copyright 2018, with permission from Elsevier.)

of experience in neuroimaging) assessed the HT2W 3D FLAIR images in consensus. MPRs were obtained using a local PACS viewer (section thickness: 0.33 mm). A systematic evaluation of the membranous labyrinth from each ear was performed following the method described by Conte et al.<sup>15</sup> In particular, the analysis was performed by taking as a reference 2 main image reconstruction planes: 1) a short-axis oblique plane parallel to the superior semicircular canal (Fig 1 and 2) an axial plane parallel to the lateral semicircular canal (Fig 2).

The observers evaluated the saccule, the utricle, and 3 ampulae of the semicircular canals as identified by Conte et al.<sup>15</sup> Each structure was assessed using an ordinal visual scale: score 0, not appreciable; score 1, visible without well-delineable boundaries; and score 2, visible with well-delineable boundaries. In addition, for visible structures (score 1 or 2), the morphology was defined as “expected” or “unexpected” according to the normal radiologic anatomy described by Conte et al.<sup>15</sup> Finally, the observers scored the quality of the MR examinations as follows: score 0, inadequate; score 1, adequate but with the presence of image degradation; and score 2, adequate.

### Data Reporting

We reported a descriptive analysis of our data because the small numbers prevented us from obtaining reliable inferential statistics. Data were analyzed using an Excel spreadsheet (Microsoft).

## RESULTS

We enrolled 10 infants (3 male, 7 female; median term equivalent age: 2 weeks [IQR: 1–5 weeks]). Five infants (50%) required

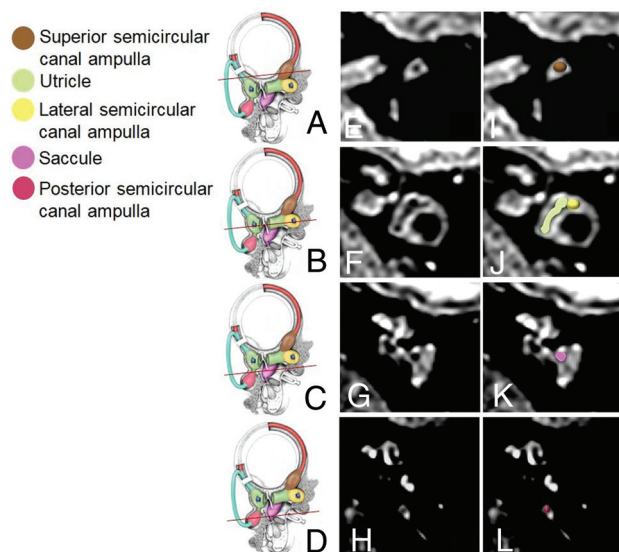


**FIG 2.** Reference working planes (A–D, asterisk) of the reformatted oblique axial MR images (E–H) parallel to the plane of the lateral semicircular canal with the corresponding colored representational images (I–L). The images were obtained from the same subject. (Reprinted from Conte G, Caschera L, Tuscano B, et al. Three-Tesla magnetic resonance imaging of the vestibular endolymphatic space: a systematic qualitative description in healthy ears. *Eur J Radiol* 2018;109:80. Copyright 2018, with permission from Elsevier.)

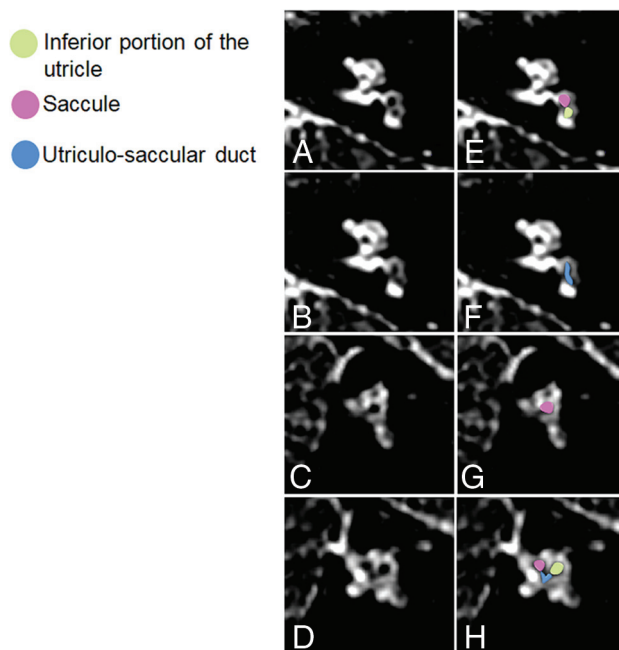


**FIG 3.** A 23-month-old female patient with extrapyramidal disorder and congenital sensorineural hearing deafness related to prematurity (born at 24 weeks of gestation). Reformatted oblique axial (A and B) and sagittal (C and D) MR images with corresponding colored representational images (E–H) showing the enlarged saccule and an elongated structure connecting the utricle and the saccule. This was interpreted as an enlarged utricular-saccular duct.

sedation during the MR imaging examination; the remaining infants were scanned during natural sleep after feeding. Nine infants were premature; congenital cytomegalovirus infection was

also diagnosed in 1 of them. Otoacoustic emissions at the neonatal hearing screening were present in all participants with the exception of 1 infant (female, 23 months old at MR imaging) who presented with extrapyramidal disorder and congenital deafness (bilateral moderately severe high-frequency sensorineural hearing loss) related to prematurity (gestational age at birth: 24 weeks).

In 4 (40%) of 10 cases, the MR examination was judged inadequate for analysis because of motion artifacts (all cases performed without sedation); 1 case (10%) was judged adequate but with the presence of image degradation (without sedation), and 5 cases (50%) were judged adequate (all cases performed with sedation). In total, 12 ears were ultimately analyzed.

The saccule was visible with well-defined boundaries in 9 ears (75%), visible without well-delineable boundaries in 1 ear (8.3%), and not visible in the 2 ears (16.7%) in the MR examination with image degradation. The morphology of the saccule was as expected in 9 (90%) of 10 ears. The saccule was enlarged in both axial and short-axis oblique planes in the left ear of the infant with congenital bilateral sensorineural hearing loss (Fig 3) resembling a saccular hydrops grade I as described in adults.<sup>16</sup> In addition, an elongated structure connecting the utricle and the saccule was identified and interpreted as an enlarged utriculo-saccular duct.<sup>17</sup> In this infant, the conventional sequences did not reveal pathologic ear and brain findings.

The utricle was visible with well-defined boundaries in 10 ears (83%) and visible without well-delineable boundaries in the 2 ears (17%) of the MR examination with image degradation. The morphology was as expected in the 12 visible utricles.

The lateral semicircular canal ampulla was visible with well-defined boundaries in 4 ears (33.3%), visible without well-defined boundaries in 1 ear (8.3%), and not visible in 7 ears (58.4%). The superior semicircular canal ampulla was visible with well-defined boundaries in 4 ears (33.3%), visible without well-defined boundaries in 2 ears (16.7%), and not visible in 6 ears (50%). The PSC ampulla was visible with well-defined boundaries in 4 ears (33.3%), visible without well-defined boundaries in 2 ears (16.7%), and not visible in 6 ears (50%). The morphology was as expected in the 17 visible ampullae.

## DISCUSSION

In this study, we describe our experience in using the noncontrast HT2W 3D FLAIR sequence for assessing the membranous labyrinth in infants. The sequence could depict the membranous labyrinth when not degraded by motion artifact. Although the sequence's long scan time (>10 minutes) led to motion artifact, all inadequate HT2W 3D FLAIR images were acquired in small infants (younger than 3 months of age) during natural sleep.

In the literature, the 4-hour-delayed contrast-enhanced HT2W 3D FLAIR sequence has been demonstrated to depict the membranous labyrinth of adults with satisfactory anatomic details.<sup>18</sup> The contrast agent gradually accumulates in the perilymph, where it reaches the maximum concentration at about 4.5 hours after IV administration. The use of 4-hour-delayed postcontrast HT2W 3D FLAIR allows for the visualization of the membranous labyrinth as a hypointense structure surrounded by the enhanced perilymph.<sup>15</sup> This sequence has largely been used in adults to describe the normal vestibular membranous labyrinth anatomy and to assess inner ear



pathologies such as Ménière disease and sudden sensorineural hearing loss.<sup>19-23</sup> In recent years, various researchers have tried to image the vestibular membranous labyrinth with noncontrast MR techniques without achieving a good differentiation between the endolymph and perilymph.<sup>24</sup> Conversely, our study showed that the membranous labyrinth can be visualized using the noncontrast HT2W 3D FLAIR sequence in infants. This finding is of importance because the contrast agent is administered with caution in this population because of potential cellular toxicity and adverse reactions.<sup>25</sup> In particular, IV administration of contrast agents is not recommended for assessing patients with congenital deafness. The radiologic work-up often includes assessment of the temporal bone using a CT scan<sup>26</sup> and of the inner ear and the CNS with noncontrast MR imaging.<sup>9-11</sup> Augmenting the MR protocol with this sequence may reveal the presence of abnormalities of the membranous labyrinth in children screened for congenital deafness, especially when conventional imaging is normal as in 1 case we demonstrated. In fact, the only patient who underwent MR imaging for congenital deafness showed an unexpected morphology of the vestibular membranous labyrinth with a hydropic saccule and a dilation of the utricular-saccular duct.

It is difficult to explain why this sequence—which is identical to that used in adults in our department—allows for the visualization of the membranous labyrinth without the need for IV contrast agent administration. Indeed, even in adults, this noncontrast HT2W 3D FLAIR sequence shows a faint signal contrast between the perilymph and the endolymph. In fact, the perilymph shows high signal because of the HT2W, but the endolymph signal is suppressed by the selective inversion time pulse based on their differing compositions. However, the membranous labyrinth remains less defined because the intrinsic high noise of the sequence lowers the contrast-to-noise ratio. This leads to our rationale for administering the contrast agent—it increases the signal of the perilymph and, as consequence, the contrast-to-noise ratio. Thus, it improves the differentiation between perilymph and endolymph (Online Fig). We theorize that the contrast-to-noise ratio is spontaneously higher in infants than in adults on the noncontrast HT2W 3D FLAIR; thus, IV contrast agent administration is not necessary to delineate the membranous labyrinth.

Other findings may further validate our hypothesis. The temporal bone is much less mineralized in infants than in adults, and the head is smaller even if the inner ear size has already reached its maximum.<sup>27</sup> These 2 factors may reduce susceptibility artifact. We also speculate that the chemical composition of the labyrinthine fluids may be different between infants and adults and thus is responsible for the spontaneous increased contrast.<sup>28</sup> Furthermore, the spontaneous contrast between the perilymph and the endolymph was also detected in the nonsedated infant whose MR examination was degraded by motion artifact, excluding a role of the administered drugs (midazolam, propofol) in the signal changes of the perilymph.

This study does have limitations. We assessed a limited cohort of participants, potentially reducing the number of anatomic variants that we observed in the imaging assessment. However, the variability of the membranous labyrinth is limited as reported in the study of Conte et al<sup>15</sup> in adults. An intraparticipant analysis comparing imaging findings before and after contrast agent

administration would have been useful for validating our results; however, the administration of a contrast agent would have been unethical without a clinical indication. There is also a study setting problem stemming from reimaging the infant after 4 hours from the base examination.

Finally, to avoid a longer scan time, we could not repeat the sequence more than once per infant, preventing us from optimizing MR parameters and addressing this critical point. Currently, the use of this sequence seems to be feasible only in sedated infants and appropriate only in the assessment of congenital sensorineural hearing loss to avoid the inappropriate prolongation of sedation; new MR technologies may overcome this drawback. Another limitation is that the 3D FLAIR MR assessment of the membranous labyrinth was performed without morphologic measurements because normal reference ranges are not available in the literature for both infants and adults.

It is well known that the bony labyrinth of the inner ear reaches its maximum in life at about 23 weeks of gestation,<sup>27</sup> and thus we supposed that the membranous labyrinth dimensions are comparable between infants and adults.

## CONCLUSIONS

Our study demonstrates that the noncontrast HT2W 3D FLAIR sequence can depict the membranous labyrinth in infants though the susceptibility to motion artifact with the lengthy scan time limits the feasibility of the sequence when infants are scanned without sedation. Further optimization of the sequence to limit scan time and improve contrast resolution may encourage its routine use in clinical practice.

## REFERENCES

1. Morton CC, Nance WE. **Newborn hearing screening—a silent revolution.** *N Engl J Med* 2006;354:2151–64 [CrossRef Medline](#)
2. Korver AMH, Smith RJH, Van Camp G, et al. **Congenital hearing loss.** *Nat Rev Dis Primers* 2017;3:16094 [CrossRef Medline](#)
3. Grosse SD, Ross DS, Dollard SC. **Congenital cytomegalovirus (CMV) infection as a cause of permanent bilateral hearing loss: a quantitative assessment.** *J Clin Virol* 2008;41:57–62 [CrossRef Medline](#)
4. Marazita ML, Ploughman LM, Rawlings B, et al. **Genetic epidemiological studies of early-onset deafness in the U.S. school-age population.** *Am J Med Genet* 1993;46:486–91 [CrossRef Medline](#)
5. Smith RJH, Bale JF Jr, White KR. **Sensorineural hearing loss in children.** *Lancet* 2005;365:879–90 [CrossRef Medline](#)
6. Snoeckx RL, Huygen PLM, Feldmann D, et al. **GJB2 mutations and degree of hearing loss: a multicenter study.** *Am J Hum Genet* 2005;77:945–57 [CrossRef Medline](#)
7. Yoshinaga-Itano C, Sedey AL, Coulter DK, et al. **Language of early- and later-identified children with hearing loss.** *Pediatrics* 1998;102:1161–71 [CrossRef Medline](#)
8. American Academy of Pediatrics, Joint Committee on Infant Hearing. **Year 2007 position statement: principles and guidelines for early hearing detection and intervention programs.** *Pediatrics* 2007;120:898–921 [CrossRef Medline](#)
9. Parry DA, Booth T, Roland PS. **Advantages of magnetic resonance imaging over computed tomography in preoperative evaluation of pediatric cochlear implant candidates.** *Otol Neurotol* 2005;26:976–82 [CrossRef Medline](#)
10. Casselman JW, Kuhweide R, Ampe W, et al. **Inner ear malformations in patients with sensorineural hearing loss: detection with**

- gradient-echo (3DFT-CISS) MRI. *Neuroradiology* 1996;38:278–86 [CrossRef Medline](#)
11. Ellul S, Shelton C, Davidson HC, et al. Preoperative cochlear implant imaging: is magnetic resonance imaging enough? *Am J Otol* 2000;21:528–33 [Medline](#)
12. Carfrae MJ, Holtzman A, Eames F, et al. 3 Tesla delayed contrast magnetic resonance imaging evaluation of Ménière's disease. *Laryngoscope* 2008;118:501–05 [CrossRef Medline](#)
13. Conte G, Lo Russo FM, Calloni SF, et al. MR imaging of endolymphatic hydrops in Ménière's disease: not all that glitters is gold. *Acta Otorhinolaryngol Ital* 2018;38:369–76 [CrossRef Medline](#)
14. Fumagalli M, Cinnante CM, Calloni SF, et al. Clinical safety of 3-T brain magnetic resonance imaging in newborns. *Pediatr Radiol* 2018;48:992–98 [CrossRef Medline](#)
15. Conte G, Caschera L, Tuscano B, et al. Three-Tesla magnetic resonance imaging of the vestibular endolymphatic space: a systematic qualitative description in healthy ears. *Eur J Radiol* 2018;109:77–82 [CrossRef Medline](#)
16. Bernaerts A, Vanspauwen R, Blaivie C, et al. The value of four stage vestibular hydrops grading and asymmetric perilymphatic enhancement in the diagnosis of Ménière's disease on MRI. *Neuroradiology* 2019;61:421–29 [CrossRef Medline](#)
17. Streeter GL. On the development of the membranous labyrinth and the acoustic and facial nerves in the human embryo. *Am J Anat* 1906;6:139–65 [CrossRef](#)
18. Naganawa S, Kawai H, Sone M, et al. Increased sensitivity to low concentration gadolinium contrast by optimized heavily T2-weighted 3D-FLAIR to visualize endolymphatic space. *MRMS* 2010;9:73–80 [CrossRef Medline](#)
19. Conte G, Caschera L, Calloni S, et al. MR imaging in Ménière disease: is the contact between the vestibular endolymphatic space and the oval window a reliable biomarker? *AJNR Am J Neuroradiol* 2018;39:2114–19 [CrossRef Medline](#)
20. Sepahdari AR, Ishiyama G, Vorasubin N, et al. Delayed intravenous contrast-enhanced 3D FLAIR MRI in Meniere's disease: correlation of quantitative measures of endolymphatic hydrops with hearing. *Clin Imaging* 2015;39:26–31 [CrossRef Medline](#)
21. Naganawa S, Yamazaki M, Kawai H, et al. Visualization of endolymphatic hydrops in Ménière's disease with single-dose intravenous gadolinium-based contrast media using heavily T2-weighted 3D-FLAIR. *Magn Reson Med Sci* 2010;9:237–42 [CrossRef Medline](#)
22. Tagaya M, Teranishi M, Naganawa S, et al. 3 Tesla magnetic resonance imaging obtained 4 hours after intravenous gadolinium injection in patients with sudden deafness. *Acta Otolaryngol* 2010;130:665–69 [CrossRef Medline](#)
23. Nakashima T, Naganawa S, Teranishi M, et al. Endolymphatic hydrops revealed by intravenous gadolinium injection in patients with Ménière's disease. *Acta Otolaryngol* 2010;130:338–43 [CrossRef Medline](#)
24. Lane JI, Witte RJ, Bolster B, et al. State of the art: 3T imaging of the membranous labyrinth. *AJNR Am J Neuroradiol* 2008;29:1436–40 [CrossRef Medline](#)
25. Maloney E, Iyer RS, Phillips GS, et al. Practical administration of intravenous contrast media in children: screening, prophylaxis, administration and treatment of adverse reactions. *Pediatr Radiol* 2019;49:433–47 [CrossRef Medline](#)
26. Conte G, Scola E, Calloni S, et al. Flat panel angiography in the cross-sectional imaging of the temporal bone: assessment of image quality and radiation dose compared with a 64 section multisection CT scanner. *AJNR Am J Neuroradiol* 2017;38:1998–2002 [CrossRef Medline](#)
27. Richard C, Courbon G, Laroche N, et al. Inner ear ossification and mineralization kinetics in human embryonic development—microtomographic and histomorphological study. *Sci Rep* 2017;7:4825 [CrossRef Medline](#)
28. Schmitt HA, Pich A, Schröder A, et al. Proteome analysis of human perilymph using an intraoperative sampling method. *J Proteome Res* 2017;16:1911–23 [CrossRef Medline](#)